Science Journal of Chemistry
2019; 7(2): 49-55
http://www.sciencepublishinggroup.com/j/sjc
doi: 10.11648/j.sjc.20190702.13
ISSN: 2330-0981 (Print); ISSN: 2330-099X (Online)

Synthesis, Characterization and *In Vitro* Cytotoxicity of Platinum (II) Complexes with Some Tetradentate Salen Ligands

Quang Trung Nguyen*, Quang Hai Lam, Phuong Nam Pham Thi, Van Tuyen Nguyen

Institute of Chemistry, Vietnam Academy of Science and Technology, Hanoi, Vietnam

Email address:
trungquang_cnhh@yahoo.com (Q. T. Nguyen)

*Corresponding author

To cite this article:
Quang Trung Nguyen, Quang Hai Lam, Phuong Nam Pham Thi, Van Tuyen Nguyen. Synthesis, Characterization and *In Vitro* Cytotoxicity of Platinum (II) Complexes with Some Tetradentate Salen Ligands. *Science Journal of Chemistry.* Vol. 7, No. 2, 2019, pp. 49-55.
doi: 10.11648/j.sjc.20190702.13

Received: May 15, 2019; **Accepted**: June 17, 2019; **Published**: July 1, 2019

Abstract: A series of platinum (II) complexes of Schiff bases derived from various salicylaldehydes with ethylenediamine were synthesized and characterized by ESI-MS, NMR and IR. The results of ESI-MS and NMR spectra data showed that the separation of hydrogen from hydoxy group and different chemical shifts of typical bondings between ligands and platinum (II) complexes evidenced for coordination of Pt (II) and tetradentate ligands. The IR spectral studies indicated the binding sites of the salen ligands with Pt (II). Their photophysical properties studied by UV-vis and luminescent spectroscopies performed the photoactivity of investigated platinum (II) complexes. The obvious effect of electron-withdrawing and – donoring substituted groups at the same position of salicyl rings and the impact of methoxy at different position of salicyl rings to their photophysical properties were studied and compared to complex 1 without substituted group. The obtained complexes were screened for their *in vitro* antitumour activities against KB and MCF-7 human cancer cell lines. Complex 4 showed the best bioactivity for both KB and MCF-7 human cancer cells with IC_{50} 1.92 μM.

Keywords: Salicylaldiminato Pt (II) Complexes, Synthesis, Photophysical Properties, Cytotoxicity

1. Introduction

The modern application of transition metal complexes as chemotherapeutic agents came from the discovery of cisplatin by Rosenberg et al. in 1965 and this discovery opened a new gate of metal-based chemotherapeutic agents which have different kinetics and mechanism of action from those of conventional organic drugs [1]. Cisplatin, carboplatin and oxaliplatin approved by FDA are platinum anticancer drugs that are used in clinic world-wide for the treatment of various cancers [2]. However, severe side effects, drug resistance and poor targeted delivery are the major problems for wider clinical application of these drugs [3]. Bioinorganic and medicinal chemists are exploring different strategies to overcome these obstacles, which includes targeted delivery of clinical drugs [4] and design of new novel platinum and non-platinum metal complexes which have different structural features and reactivities [5].

Schiff bases are considered as a very important class of organic compounds which have wide applications in many biological aspects [6]. Schiff base ligands can form quite stable complexes with many transition metals, with different oxidation states, coordination numbers and geometries [7]. Schiff base complexes are used as model molecules for biological oxygen carrier systems. Some of these complexes have applications in analytical fields [8]. Recently some tetradentate salicylaldiminato Pt (II) complexes were synthesized and estimated for their photophysical properties [9-14] and cytotoxicity [15-18]. Because of tetradentate salicylaldiminato Pt (II) complexes' potential in chemotherapy for various human cancer cell lines, in this research we continue to study on Pt (II) complexes of tetradentate salicylaldimine ligands derived from various salicylaldehydes with ethylenediamine and estimate their photophysical properties and *in vitro* cytotoxicity for KB and MCF-7 human cancer cell lines as well.

2. Experimental and Results

2.1. Chemicals and Instrumentation

All chemicals used in the synthesis were of reagent grade and obtained from commercial companies. Solvents were purified by standard procedures before using. IR spectra at 4000-400 cm^{-1} were recorded on Perkin-Elmer Spectrum Two. ^{1}H and ^{13}C-NMR were obtained on Bruker Avance 500 at 500 and 150 MHz with TMS as internal standard and chemical shifts (δ) were reported in ppm. ESI-MS was determined on Agilent 6310 Ion Trap in analytical center of Vietnam Institute of Chemistry. Reactions were all monitored by TLC, performed on silica gel plates 60 F254 (Merck, Germany). Visualization on TLC was achieved by UV lamb.

2.2. Synthesis of Salen Ligands

Generally salen ligands were synthesized following the published paper [19] by mixing two equivalents of salicylaldehyde (or derivatives) with one equivalent of ethylenediamine in ethanol at room temperature that resulted in yellow colored precipitate of respective salen derivatives. The precipitate was filtered, washed with cold ethanol and dried under reduced pressure. Each of the ligand was characterized by ESI-MS, IR, ^{1}H and ^{13}C NMR spectra and the results are consistent with their structures.

N, N'-Bis (salicylidene) ethylene diimine (salenH_2)

Yellow solid product, yield 93%. ESI-MS (m/z) 268.9 $[M+H]^+$. IR (KBr, cm^{-1}): 2900 (ν, C–H); 2549 (ν, O–H); 1636 (ν, C═N); 1497 (ν, C═C); 1283 (ν, C–N); 1199 (ν, C–O); 1042; 856; 742 (δ, C–H). ^{1}H-NMR ($CDCl_3$, ppm, Hz): δ 13.18 (s, 2H, 2OH); 8.35 (s, 2H, 2CH=N); 7.28 (dt, *J* = 8.0; 2.0, 2H, Ar–H); 7.21 (dd, *J* = 7.5; 2.0, 2H, Ar–H); 6.93 (d, *J* = 8.0, 2H, Ar–H); 6.84 (dt, *J* = 7.5; 1.0, 2H, Ar–H); 3.93 (s, 4H, CH_2–CH_2). ^{13}C-NMR ($CDCl_3$, ppm): δ 166.51 (2C, 2C−O); 161.03 (2C, 2C=N); 132.40 (2C, C_{Ar}); 131.49 (2C, C_{Ar}); 118.69 (2C, C_{Ar}); 118.67 (2C, C_{Ar}); 116.97 (2C, C_{Ar}); 59.75 (2C, CH_2–CH_2).

N, N'-Bis (5-fluorosalicylidene) ethylene diimine (5-FsalenH_2)

Yellow solid product, yield 95%. ESI-MS (m/z) 304.9 $[M+H]^+$. IR (KBr, cm^{-1}): 2911 (ν, C–H); 2571 (ν, O–H); 1634 (ν, C═N); 1498 (ν, C=C); 1364; 1272 (ν, C–N); 1225 (ν, C–O); 1041; 828; 782 (δ, C–H). ^{1}H-NMR ($CDCl_3$, ppm): δ 12.85 (s, 2H, 2OH); 8.30 (s, 2H, 2CH=N); 7.02 (m, 2H, Ar–H); 6.93 (dd, *J* = 8.5; 3.0, 2H, Ar–H); 6.89 (dd, *J* = 8.0; 4.0, 2H, Ar–H); 3.96 (s, 4H, CH_2–CH_2). ^{13}C-NMR ($CDCl_3$, ppm): δ 165.58 and 165.56 (2C, 2C–O); 154.60 (2C, 2C=N); 157.25 and 156.48 (2C, 2C–F); 119.65 and 119.47 (2C, C_{Ar}); 118.48 and 118.43 (2C, C_{Ar}); 118.17 and 118.11 (2C, C_{Ar}); 116.61 and 116.43 (2C, C_{Ar}); 59.71 (2C, CH_2–CH_2).

N, N'-Bis (3-methoxysalicylidene) ethylene diimine (3-MeOsalenH_2)

Yellow solid product, yield 91%. ESI-MS (m/z) 329.0 $[M+H]^+$. IR (KBr, cm^{-1}): 2921 (ν, C–H); 2555 (ν, O–H); 1633 (ν, C═N); 1470 (ν, C═C); 1296 (ν, C–N); 1250 (ν, C–O); 1081; 963; 741 (δ, C–H). ^{1}H-NMR ($CDCl_3$, ppm): δ 13.55 (s, 2H, 2OH); 8.32 (s, 2H, 2CH=N); 6.91 (dd, *J* = 8.0; 1.5, 2H, Ar–H); 6.85 (dd, *J* = 8.0; 1.5, 2H, Ar–H); 6.77 (t, *J* = 8.0, 2H, Ar–H); 3.95 (s, 4H, CH_2–CH_2); 3.88 (s, 6H, 2MeO). ^{13}C-NMR ($CDCl_3$, ppm): δ 166.68 (2C, 2C–O); 151.49 (2C, 2C=N); 148.34 (2C, 2C–OMe); 123.21 (2C, C_{Ar}); 118.49 (2C, C_{Ar}); 118.06 (2C, C_{Ar}); 114.23 (2C, C_{Ar}); 59.50 (2C, CH_2–CH_2); 56.11 (2C, 2MeO).

N, N'-Bis (4-methoxysalicylidene) ethylene diimine (4-MeOsalenH_2)

Yellow solid product, yield 91%. ESI-MS (m/z) 329.0 $[M+H]^+$. IR (KBr, cm^{-1}): 2927 (ν, C–H); 2551 (ν, O–H); 1620 (ν, C═N); 1512 (ν, C=C); 1285 (ν, C–N); 1223 (ν, C–O); 1114; 964; 852, 800 (δ, C–H). ^{1}H-NMR ($CDCl_3$, ppm): δ 13.68 (s, 2H, 2OH); 8.20 (s, 2H, 2CH=N); 7.08 (d, *J* = 8.5, 2H, Ar–H); 6.41 (d, *J* = 2.5, 2H, Ar–H); 6.37 (dd, *J* = 8.5; 2.5, 2H, Ar–H); 3.85 (s, 4H, CH_2–CH_2); 3.79 (s, 6H, 2MeO). ^{13}C-NMR ($CDCl_3$, ppm): δ 165.43 (2C, 2C−O); 164.65 (2C, 2C– OMe); 163.53 (2C, 2C=N); 132.71 (2C, C_{Ar}); 112.36 (2C, C_{Ar}); 106.43 (2C, C_{Ar}); 101.16 (2C, C_{Ar}); 58.85 (2C, CH_2–CH_2); 55.34 (2C, 2MeO).

N, N'-Bis (5-methoxysalicylidene) ethylene diimine (5-MeOsalenH_2)

Yellow solid product, yield 92%. ESI-MS (m/z) 329.0 $[M+H]^+$. IR (KBr, cm^{-1}): 2937 (ν, C–H); 2572 (ν, O–H); 1639 (ν, C═N); 1492 (ν, C=C); 1276 (ν, C–N); 1159 (ν, C–O); 1031; 829; 784 (δ, C–H). ^{1}H-NMR ($CDCl_3$, ppm): δ 12.68 (s, 2H, 2OH); 8.30 (s, 2H, 2CH=N); 6.90 (dd, *J* = 9.0; 3.0, 2H, Ar–H); 6.87 (d, *J* = 9.0, 2H, Ar–H); 6.73 (d, *J* = 3.0, 2H, Ar–H); 3.94 (s, 4H, CH_2–CH_2); 3.75 (s, 6H, 2MeO). ^{13}C-NMR ($CDCl_3$, ppm): δ 166.27 (2C, 2C−O); 155.17 (2C, 2C=N); 152.06 (2C, 2C–OMe); 119.56 (2C, C_{Ar}); 118.27 (2C, C_{Ar}); 117.70 (2C, C_{Ar}); 114.98 (2C, C_{Ar}); 59.85 (2C, CH_2–CH_2); 55.95 (2C, 2MeO).

N, N'-Bis (6-methoxysalicylidene) ethylene diimine (6-MeOsalenH_2)

Yellow solid product, yield 91%. ESI-MS (m/z) 329.0 $[M+H]^+$. IR (KBr, cm^{-1}): 2937 (ν, C–H); 2532 (ν, O–H); 1627 (ν, C═N); 1462 (ν, C=C); 1295 (ν, C–N); 1250 (ν, C–O); 1099; 837; 780 (δ, C–H); 722. ^{1}H-NMR ($CDCl_3$, ppm): δ 14.18 (s, 2H, 2OH); 8.80 (s, 2H, 2CH=N); 7.19 (t, *J* = 8.5, 2H, Ar–H); 6.51 (d, *J* = 8.5, 2H, Ar–H); 6.25 (d, *J* = 8.5, 2H, Ar–H); 3.88 (s, 4H, CH_2–CH_2); 3.78 (s, 6H, 2MeO). ^{13}C-NMR ($CDCl_3$, ppm): δ 163.80 (2C, 2C–O); 162.63 (2C, 2C=N); 159.64 (2C, 2C–OMe); 133.46 (2C, C_{Ar}); 110.24 (2C, C_{Ar}); 108.08 (2C, C_{Ar}); 99.78 (2C, C_{Ar}); 59.65 (2C, CH_2–CH_2); 55.57 (2C, 2MeO).

2.3. Synthesis of Salen Pt (II) Complexes

Pt (II)-salen derivatives were synthesized and characterized following a general procedure as described previously [20]. In general, for the synthesis of Pt (II)-salen derivatives, the respective salen ligand derivatives were dissolved DMSO and then mixed with equivalent amount of K_2PtCl_4 (200 mg, 0.48 mmol) in DMSO. Then aqueous saturated solution of Na_2CO_3 (52 mg, 0.48 mmol) was added. The reaction mixture was stired continuously and refluxed for 3 h. After cooling to room temperature the yellow

precipitate was filtered and washed by distilled water and cold ethenol, then dried in reduced vacuo to afford a yellow solid product. The products were isolated, recrystallized from ethyl ether and characterized by mass spectral (ESI-MS), ^{1}H and ^{13}C-NMR, and IR spectra.

[Pt (II) (salen)] (1): Yellow solid, yield 67.5%. ESI-MS (m/z) 462.1 $[M+H]^+$. IR (KBr, cm^{-1}): 3022 (ν, C–H); 1621 (ν, C═N); 1530 (ν, C=C); 1439; 1309; 1192 (ν, C–N); 1127 (ν, C–O); 1081; 846; 742 (δ, C–H); 611 (Pt−O); 417 (Pt−N). ^{1}H-NMR (DMSO-d_6, ppm): 8.54 (s, 2H, 2CH=N); 7.50 (d, J = 7.5 Hz, 2H, Ar–H); 7.43 (t, J = 7.0, 2H, Ar–H); 6.91 (d, J = 8.5, 2H, Ar–H); 6.61 (t, J = 7.0, 2H, Ar–H); 3.82 (s, 4H, CH_2–CH_2). ^{13}C-NMR (DMSO-d_6, ppm): δ 162.45 (2C, 2C−O); 155.98 (2C, 2C=N); 133.70 (2C, C_{Ar}); 133.48 (2C, C_{Ar}); 122.28 (2C, C_{Ar}); 120.94 (2C, C_{Ar}); 115.48 (2C, C_{Ar}); 60.92 (2C, CH_2–CH_2).

[Pt (II) (5-Fsalen)] (2): Yellow solid, yield 68.5%. ESI-MS (m/z) 497.9 $[M+H]^+$. IR (KBr, cm^{-1}): 3019 (ν, C–H); 1612 (ν, C═N); 1545 (ν, C=C); 1472; 1313; 1221 (ν, C–N); 1127 (ν, C–O); 1021; 971; 807 (δ, C–H); 618 (Pt−O); 434 (Pt−N). ^{1}H-NMR (DMSO-d_6, ppm): 8.22 (s, 2H, 2CH=N); 7.27 (m, 2H, Ar–H); 7.18 (dd, J = 9.0; 3.5 Hz, 2H, Ar–H); 6.91 (dd, J = 9.5; 4.5, 2H, Ar–H); 4.46 (s, 4H, CH_2–CH_2). ^{13}C-NMR (DMSO-d_6, ppm): δ 162.62 (2C, 2C−O); 157.98 (2C, 2C=N); 153.83 and 151.98 (2C, 2C–F); 123.25 and 123.06 (2C, C_{Ar}); 120.24 and 120.18 (2C, C_{Ar}); 118.43 and 118.36 (2C, C_{Ar}); 117.18 and 117.00 (2C, C_{Ar}); 60.49 (2C, CH_2–CH_2).

[Pt (II) (3-MeOsalen)] (3): Yellow solid, yield 66.0%. ESI-MS (m/z) 522.0 $[M+H]^+$. IR (KBr, cm^{-1}): 3011 (ν, C–H); 1604 (ν, C═N); 1548 (ν, C=C); 1466; 1325; 1247 (ν, C–N); 1126 (ν, C–O); 1031; 977; 733 (δ, C–H); 631 (Pt−O); 433 (Pt−N). ^{1}H-NMR (DMSO-d_6, ppm): 8.52 (s, 2H, 2CH=N); 7.08 (dd, J = 8.0; 1.5, 2H, Ar–H); 7.04 (dd, J = 8.0; 1.5, 2H, Ar–H); 6.55 (t, J = 8.0, 2H, Ar–H); 3.81 (s, 4H, CH_2–CH_2); 3.77 (s, 6H, 2 MeO). ^{13}C-NMR (DMSO-d_6, ppm): δ 156.00 (2C, 2C−O); 153.53 (2C, 2C=N); 151.32 (2C, 2C–OMe); 124.89 (2C, C_{Ar}); 121.83 (2C, C_{Ar}); 114.51 (2C, C_{Ar}); 113.33 (2C, C_{Ar}); 60.92 (2C, CH_2–CH_2); 55.18 (2C, 2 MeO).

[Pt (II) (4-MeOsalen)] (4): Light yellow solid, yield 65.5%. ESI-MS (m/z) 522.0 $[M+H]^+$. IR (KBr, cm^{-1}): 3020 (ν, C–H); 1600 (ν, C═N); 1533 (ν, C=C); 1456; 1317; 1228 (ν, C–N); 1124 (ν, C–O); 1025; 980; 828; (δ, C–H); 625 (Pt−O); 432 (Pt−N). ^{1}H-NMR (DMSO-d_6, ppm): 8.02 (s, 2H, 2CH=N); 7.22 (d, J = 9.0, 2H, Ar–H); 6.44 (d, J = 2.5, 2H, Ar–H); 6.25 (dd, J = 9.0; 2.0, 2H, Ar–H); 4.32 (s, 4H, CH_2–CH_2); 3.73 (s, 6H, 2 MeO). ^{13}C-NMR (DMSO-d_6, ppm): δ 165.41 (2C, 2C–OMe); 163.13 (2C, 2C−O); 161.81 (2C, 2C=N); 136.03 (2C, C_{Ar}); 113.48 (2C, C_{Ar}); 107.37 (2C, C_{Ar}); 100.75 (2C, C_{Ar}); 60.53 (2C, CH_2–CH_2); 55.39 (2C, 2 MeO).

[Pt (II) (5-MeOsalen)] (5): Yellow solid, yield 67.5%. ESI-MS (m/z) 522.0 $[M+H]^+$. IR (KBr, cm^{-1}): 3002 (ν, C–H); 1607 (ν, C═N); 1539 (ν, C=C); 1474; 1299; 1220 (ν, C–N); 1148 (ν, C–O); 1033; 928; 829 (δ, C–H); 613 (Pt−O); 427 (Pt−N). ^{1}H-NMR (DMSO-d_6, ppm): 8.47 (s, 2H, 2CH=N); 7.14 (dd, J = 9.5; 3.5, 2H, Ar–H); 7.00 (d, J = 3.0, 2H, Ar–H); 6.84 (d, J = 9.5, 2H, Ar–H); 3.80 (s, 4H, CH_2–CH_2); 3.69 (s, 6H, 2 MeO). ^{13}C-NMR (DMSO-d_6, ppm): δ 157.73 (2C, 2C−O); 155.41 (2C, 2C=N); 149.23 (2C, 2C–OMe); 123.22 (2C, C_{Ar}); 121.67 (2C, C_{Ar}); 120.85 (2C, C_{Ar}); 113.81 (2C, C_{Ar}); 60.95 (2C, CH_2–CH_2); 55.53 (2C, 2 MeO).

[Pt (II) (6-MeOsalen)] (6): Yellow solid, yield 67.0%. ESI-MS (m/z) 522.0 $[M+H]^+$. IR (KBr, cm^{-1}): 3006 (ν, C–H); 1607 (ν, C═N); 1545 (ν, C=C); 1455; 1317; 1254 (ν, C–N); 1106 (ν, C–O); 1040; 778 (δ, C–H); 623 (Pt−O); 434 (Pt−N). ^{1}H-NMR (DMSO-d_6, ppm): 8.77 (s, 2H, 2CH=N); 7.29 (t, J = 8.0, 2H, Ar–H); 6.51 (d, J = 3.5, 2H, Ar–H); 6.20 (d, J = 8.0, 2H, Ar–H); 3.82 (s, 10H, CH_2–CH_2 and 2 MeO). ^{13}C-NMR (DMSO-d_6, ppm): δ 163.21 (2C, 2C−O); 159.36 (2C, 2C=N); 149.78 (2C, 2C–OMe); 132.83 (2C, C_{Ar}); 114.25 (2C, C_{Ar}); 112.43 (2C, C_{Ar}); 96.98 (2C, C_{Ar}); 61.58 (2C, CH_2–CH_2); 55.84 (2C, 2 MeO).

2.4. Photophysical Properties

The UV-Visible absorption spectra of investigated platinum (II) complexes were recorded in DCM (dichlorometane) solutions (2×10^{-5} M) on Perkin Elmer Lambda UV-35 spectrophotometer. The luminescent spectra of the solutions were measured on Horiba Fluorolog spectrofluorometer at room temperature. The received photophysical data were collected in Table 1.

Table 1. *Photophysical data of investigated Pt (II) complexes with salen ligands.*

Complex	λ_{abs} (nm) (ε, M^{-1} cm^{-1})			λ_{em} (λ_{exc}) (nm)
	π–π*	n–π*	MLCT	
1	317 (20, 415)	342 (24, 840)	422 (9, 200)	549 (422)
2	292 (11, 045)	350 (5, 055)	429 (6, 720)	572 (429)
3	300 (24, 210)	362 (5, 930)	424 (8, 405)	561 (424)
4	305 (29, 615)	368 (9, 975)	398 (6, 960)	525 (398)
5	320 (14, 130)	360 (10, 980)	446 (8, 740)	601 (446)
6	325 (19, 725)	358 (15, 050)	410 (5, 585)	545 (410)

2.5. In vitro Cytotoxicity Assay

The cytotoxicity of studied Pt (II) complexes was estimated by using MTT assay as described previously [21]. In brief, human epidermoid carcinoma cells (KB) or breast cancer cells (MCF-7) were cultured and maintained in DMEM which was added with 10% FBS (Fetal Bovine Serum) and 1% penicillin streptomycin at 37ºC in humidified atmosphere with 5% CO_2 and 95% air. Testing samples of Pt (II) complexes were dissolved in DMSO to give various concentrations of 0–128 μg/ml. Approximately 10,000 cancer cells were seeded into each well of a 96 well micro titer plate and incubated 24 h. Then 10 μL solution containing various

concentrations of different Pt (II)-salen complexes and 190 µL DMEM solution containing cancer cells were added into each wells and incubated for additional 72 h under standard growing condition. The cell viability was analyzed by using MTT assay based on the absorbance of the lysates at 540 nm on Genios TECAN spectrophotometter. The percent viable cells were plotted as a function of concentration to determine the IC_{50} values. The each experiment was carried out triplicate. The obtained IC_{50} values of studied complexes were presented in Table 2.

Table 2. *The in vitro cytotoxcity of Pt (II) complexes with salen ligands.*

Complex	IC_{50} (µM)	
	KB	MCF-7
1	3.15 [20]	13.45 [20]
2	8.05	8.05
3	5.37	7.68
4	1.92	1.92
5	2.88	3.26
6	7.68	25.53
Ellipticine	1.14	2.03

3. Discussion

3.1. Synthesis and Characterization

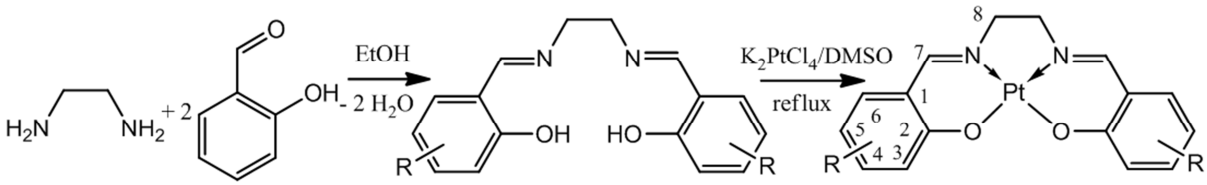

Figure 1. *Synthesis of salen ligands and complexes.*

Table 3. *Salen ligands and their Platinum (II) complexes.*

R	Ligand	Complex
H	$SalenH_2$	[Pt (II) (salen)] (1)
5-F	5-FsalenH2	[Pt (II) (5-Fsalen)] (2)
3-MeO	3-$MeOsalenH_2$	[Pt (II) (3-MeOsalen)] (3)
4-MeO	4-$MeOsalenH_2$	[Pt (II) (4-MeOsalen)] (4)
5-MeO	5-$MeOsalenH_2$	[Pt (II) (5-MeOsalen)] (5)
6-MeO	6-$MeOsalenH_2$	[Pt (II) (6-MeOsalen)] (6)

Firstly, the N, N'-bis (salicylidene)-1, 2-ethylenediimine ligands were synthesized in high yields (91−95%). The commercial 1, 2-ethylenediamine was reacted with two equivalents of salicylaldehydes in ethanol as solvent at room temperature. The productive precipitates were collected and washed by cold ethanol to afford yellowish solids. Their ESI-MS spectra received were in good agreement with their suggested formula weights. The bands at about 2532-2619 cm^{-1} in the IR spectra of ligands can be assigned to the O−H stretching frequencies. The vibration band of C=N was appeared in the frequencies of 1577-1639 cm^{-1}. The characteristic bands found at about 1261-1296 and 1159-1250 cm^{-1} can belong to C−N and C−O stretching vibrations respectively (Table 4). In ^{1}H-NMR spectra recorded in $CDCl_3$, the typical signals at about 12.68-14.18 ppm can be assigned to the OH proton peaks. The signals at 8.20-8.80 ppm can assure the ligand formulation bonding CH=N. The proton peaks of ethylene were found at 3.85-3.96 ppm. The substituted groups at salicylidene moiety afforded the characteristic signals in ^{1}H-NMR. The proton signals of salicyl ring with fluoro at 5-position observed at 6.89-7.02 ppm were in multilets. The proton signals of MeO groups of $MeOsalenH_2$ ligands were appeared as a singlet in the field of 3.75-3.88 ppm (Table 5). ^{13}C-NMR spectra showed the characteristic peaks at about 156.00-166.68 ppm for C−O, 151.49-163.53 ppm for C=N and 58.85-59.85 ppm for CH_2CH_2 carbon signals. All carbon peaks of salicyl ring with fluoro at 5-positon were appeared in double ones. The carbon signals of MeO groups of $MeOsalenH_2$ ligands were at about 55.34-56.11 ppm (Table 6).

Then a series of Pt (II) complexes were prepared in moderate yields (65.5−68.5%) between synthetic salen ligands and K_2PtCl_4 in mild condition [Figure 1]. Their ESI-MS spectra were suitable to their proposed molecular formulations (Table 3). In IR spectra, the characteristic peaks of ligands were found at 1600-1621 cm^{-1} for C=N, 1192-1254 cm^{-1} for C−N and 1106-1248 cm^{-1} for C−O stretching vibrations. The vibrations of these bongdings were shifted to higher fields in coordination. New vibrations of Pt–N and Pt–O for the coordination between Pt (II) and tetradentate salen ligands were observed at 611-631 and 417-434 cm^{-1} respectively (Table 4).

Table 4. *Main IR absorption of ligands and Pt (II) complexes (cm^{-1}).*

Compound	$\upsilon_{(O-H)}$ (cm^{-1})	$\upsilon_{(C=N)}$ (cm^{-1})	$\upsilon_{(C-N)}$ (cm^{-1})	$\upsilon_{(C-O)}$ (cm^{-1})	$\upsilon_{(Pt-N)}$ (cm^{-1})	$\upsilon_{(Pt-O)}$ (cm^{-1})
$SalenH_2$	2549	1636	1283	1199	-	-
5-FsalenH2	2571	1634	1272	1225	-	-
3-$MeOsalenH_2$	2555	1633	1296	1250	-	-

Compound	$\upsilon_{(O-H)}$ (cm^{-1})	$\upsilon_{(C=N)}$ (cm^{-1})	$\upsilon_{(C-N)}$ (cm^{-1})	$\upsilon_{(C-O)}$ (cm^{-1})	$\upsilon_{(Pt-N)}$ (cm^{-1})	$\upsilon_{(Pt-O)}$ (cm^{-1})
4-MeOsalenH_2	2551	1620	1285	1223	-	-
5-MeOsalenH_2	2571	1639	1276	1159	-	-
6-MeOsalenH_2	2531	1627	1295	1250	-	-
1	-	1621	1192	1127	611	417
2	-	1612	1221	1127	618	434
3	-	1604	1247	1126	631	433
4	-	1600	1228	1124	625	432
5	-	1607	1220	1148	613	427
6	-	1607	1254	1106	623	434

In ^{1}H-NMR spectra of Pt (II) complexes recorded in DMSO-d_6, there were no signal for OH groups in low field showing that the separation of H in coordination. Other typical proton signals were found in a singlet at 8.02-8.77 ppm for CH=N and a singlet at 3.80-4.46 ppm for CH_2CH_2 groups. The protons of complex 2 salicyl ring with fluoro at 5-position was observed in multilets. The proton peaks of MeO group in [Pt (II) MeOsalen] complexes were appeared as a singlet at 3.69-3.82 ppm (Table 5).

Table 5. *Typical ^{1}H-NMR signals of salen ligands and Pt (II) complexes (ppm).*

Compound	$\delta_{(OH)}$ (ppm)	$\delta_{(CH=N)}$ (ppm)	$\delta_{(CH2CH2)}$ (ppm)	$\delta_{(MeO)}$ (ppm)
SalenH_2	13.18	8.35	3.93	-
5-FsalenH2	12.85	8.30	3.96	-
3-MeOsalenH_2	13.55	8.32	3.95	3.88
4-MeOsalenH_2	13.68	8.20	3.85	3.79
5-MeOsalenH_2	12.68	8.30	3.94	3.75
6-MeOsalenH_2	14.18	8.80	3.88	3.78
1	-	8.54	3.82	-
2	-	8.22	4.46	-
3	-	8.52	3.81	3.77
4	-	8.02	4.32	3.73
5	-	8.47	3.80	3.69
6	-	8.77	3.82	3.82

In ^{13}C-NMR spectra, the typical carbon signals presentating for C−O were found at 156.00-163.21 ppm, C=N at 153.53-161.81 and CH_2CH_2 at 60.49-61.58 ppm. Other carbon signals of salicylidene moiety with fluoro at 5-position in complex 2 were observed as double peaks at about 117.00-153.83 ppm. The carbon signals of MeO groups in [Pt (II)(MeOsalen)] complexes were appeared at 55.18-55.84 ppm (Table 6).

Table 6. *Typical ^{13}C-NMR signals of salen ligands and Pt (II) complexes (ppm).*

Compound	$\delta_{(OH)}$ (ppm)	$\delta_{(CH=N)}$ (ppm)	$\delta_{(CH2CH2)}$ (ppm)	$\delta_{(MeO)}$ (ppm)
SalenH_2	166.51	161.03	59.75	-
5-FsalenH2	165.58 and 165.56	154.60	59.71	-
3-MeOsalenH_2	166.68	151.49	59.50	56.11
4-MeOsalenH_2	165.43	163.53	58.85	55.34
5-MeOsalenH_2	166.27	155.17	59.85	55.95
6-MeOsalenH_2	163.80	162.63	59.65	55.57
1	162.45	155.98	60.92	-
2	162.62	157.98	60.49	-
3	156.00	153.53	60.92	55.18
4	163.13	161.81	60.53	55.39
5	157.73	155.41	60.95	55.53
6	163.21	159.36	61.58	55.84

3.2. Photophysical Properties

The photophysical data of Pt (II) complexes in dilute DCM solutions were presented in Table 1.

When dissolved in DCM, Pt (II) complexes gave yellow solutions and exhibited UV-Visible absorption spectra with λ_{max} at about 292-446 nm of three bands. Two bands at 292-325 and 342-368 nm could featured for high-energy intra-ligand absorption of $\pi\rightarrow\pi^*$ and $n\rightarrow\pi^*$ transitions respectively and a low-energy metal-to-ligand charge transfer (MLCT) absorption must be at 398-446 nm probably (Figure 2). Compared to complex 1, both electron-withdrawing and -donoring substituted groups at 5-position of salicyl rings of complex 2 and 5 respectively shifted MLCT absorption bands to longer wavelengths. Methoxy group at different position of salicyl rings also perform obvious impact to MLCT absorption wavelengths of investigated complexes. Methoxy group at 3 or 5-position shifted wavelength to longer range while methoxy at 4 or 6-position moved the wavelength to shoter band (Table 1).

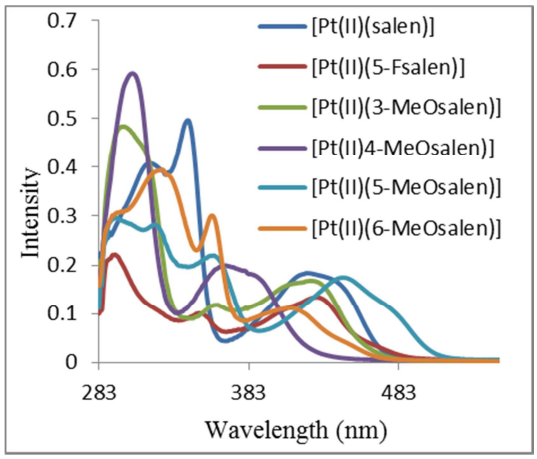

Figure 2. *UV-Visible absorption spectra.*

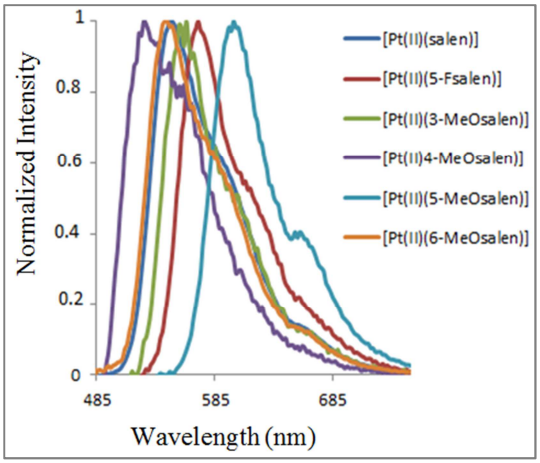

Figure 3. *Emission spectra of Pt (II) complexes.*

The emission spectra in solution of these complexes exhibited λ_{max} at about 525-601 nm. The substituted group of fluoro at salicyl ring 5-position may shift emission spectra of complex 2 to red region. Methoxy group at different positions of salicyl ring could also affect to Pt (II) complexes' emission wavelengths. Methoxy group at 3- or 5-position of salicyl ring could shift emission band to red range and methoxy group at salicyl ring 4- or 6- postion must shift emission band to blue region (Figure 3).

3.3. In Vitro Cytotoxicity

In order to observe possible structure-activity relationships, the *in vitro* cytotoxicity of obtained platinum (II) complexes was evaluated against two human cancer cell lines of KB and MCF-7. The IC_{50} values (the concentration that inhibited in 50% the cellular proliferation) was presented in Table 2. It was noted that all investigated platinum (II) complexes have antiproliferative effectivity with low IC_{50} values (< 50 µM). The effect of the substituted groups of studied ligands to complexes' cytotoxicity was quite obvious. In details, electron donoring methoxy at salicyl ring 5-position in complex 5 gave better activity than electron withdrawing fluoro in complex 2. The methoxy at different position of salicylidene moiety also showed the different effect on both human cancer cell lines. Methoxy at 4- or 5-position afforded the better results the one at 3- or 6-position. Compared to the standard anticancer compound, complex 4 gave the anticancer activity with IC_{50} = 1.92 µM for both KB and MCF-7 similar to the activity of standard ellipticine, IC_{50} = 1.14 µM for KB and 2.03 for MCF-7. It can be seen that the *in vitro* cytotoxicity of this series of platinum (II) complexes increases in the sequence 2 < 6 < 3 < 1 < 5 < 4 for BK and 6 < 1 < 2 < 3 < 5 < 4 for MCF-7 cancer cell lines.

4. Conclusions

In this study, a series of platinum (II) complexes with salen ligands were synthesized and characterized by ESI-MS, IR and NMR spectroscopies. The photophysical properties estimated by UV-Visible absorption and emission spectra show that electron-withdrawing or -donoring substituted groups at 5-position of salicyl rings shifted MLCT absorption and emission bands to longer wavelengths. Methoxy group at different position of salicyl rings also perform obvious effect to MLCT absorption and emission wavelengths of investigated complexes. Methoxy group at 3 or 5-position shifted wavelength to longer range while methoxy at 4 or 6-position moved the wavelength to shoter one. The biological activity of all complexes were examined against human cancer cell lines of KB and MCF-7, the results showed that all complexes have influenced KB and MCF-7 cell lines with low IC_{50} values (< 50 µM). Complex 4 gave the best activity for both KB and MCF-7 with IC_{50}=1.92 µM which was similar to the cytotoxicity of standard anticancer compound, ellipticine, 1.14 and 2.03 µM respectively.

Acknowledgements

This work is financially supported by Vietnam Academy of Science and Technology under grant number VAST04.01/17−18.

References

[1] N. Muhammad, Z. Guo. Metal-based anticancer chemotherapeutic agents. Cur. Op. Chem. Biol. 19 (2014) 144–153.

[2] U. Kalinowska-Lis, J. Ochocki, K. Matlawska-Wasowska. Trans geometry in platinum antitumor complexes. Coor. Chem. Rev. 252 (2008) 1328–1345.

[3] P. Heffeter, U. Jungwirth, M. Jakupec, C. Hartinger, M. Galanski, L. Elbling, M. Micksche, B. Keppler, W. Berger. Resistance against novel anticancer metal compounds: Differences and similarities. Drug Resis. Upd. 11 (2008) 1–16.

[4] Anne-Laure Laine, C. Passirani. Novel metal-based anticancer drugs: a new challenge in drug delivery. Cur. Op. Pharm. 12 (2012) 420–426.

[5] Pieter CA Bruijnincx, Peter J Sadler. New trends for metal complexes with anticancer activity. Cur. Op. Chem. Biol. 12 (2008) 197–206.

[6] Cleiton M. da Silva, Daniel L. da Silva, Luzia V. Modolo, Rosemeire B. Alves, Maria A. de Resende, Cleide V. B. Martins, Ângelo de Fátima. Schiff bases: A short review of their antimicrobial activities. J. Adv. Research 2 (2011) 1−8.

[7] K. C. Gupta, A. K. Sutar. Catalytic activities of Schiff base transition metal complexes. Coor. Chem. Rev. 252 (2008) 1420–1450.

[8] A. Erxleben. Transition metal salen complexes in bioinorganic and medicinal chemistry. Inorg. Chim. Acta 472 (2018) 40–57.

[9] Y. Zhang, F. Meng, C. You, S. Yang, W. Xiong, Y. Wang, S. Su, W. Zhu, Achieving NIR emission for tetradentate platinum (II) salophen complexes by attaching dual donor-accepter frameworks in the heads of salophen, Dyes and Pigments 138 (2017) 100−106.

[10] Y. Zhang, Z. Yin, F. Meng, J. Yu, C. You, S. Yang, H. Tan, W. Zhu, S. Su, Tetradentate Pt (II) 3, 6-substitued salophen complexes: Synthesis and tuning emission from deep-red to near infrared by appending donoracceptor framework, Organic Electronics 50 (2017) 317−324.

[11] Hirohiko Houjou, Yuki Hoga, Yi-Lan Ma, Hiroto Achira, Isao Yoshikawa, Toshiki Mutai, Kazunari Matsumura, Dinuclear fused salen complexes of group-10 metals: Peculiarity of the crystal structure and near-infrared luminescence of a bis (Pt-salen) complex, Inorg. Chim. Acta 461 (2017) 27–34.

[12] H. Achira, Y. Hoga, I. Yoshikawa, T. Mutai, K. Matsumura, H. Houjou, Effects of a semiflexible linker on the mechanochromic photoluminescence of bis (Pt-salen) complex, Polyhedron 113 (2016) 123–131.

[13] J. Zhang, G. Dai, F. Wu, D. Li, D. Gao, H. Jin, S. Chen, X. Zhu, C. Huang, D. Han. Efficient and tunable phosphorescence of new platinum (II) complexes based on the donor–π–acceptor Schiff bases. J. Photochem. Photobiol A: Chem. 316 (2016) 12–18.

[14] M. Hashemi, Z. Solati, A. Ghodsi, S. Ahmadian. Azo-substituted Schiff base complex of Pt (II): Synthesis, characterization, DFT and TD-DFT study. Syn. Metals 210 (2015) 398–403.

[15] Peng Wu, Dik-Lung Ma, Chung-Hang Leung, Siu-Cheong Yan, Nianyong Zhu, R. Abagyan, Chi-Ming Che. Stabilization of G-quadruplex DNA with platinum (II) Schiff base complexes: Luminescent probe and down-regulation of c-myc oncogene expression. Chem. Eur. J. 15 (2009) 13008 –13021.

[16] M. Proetto, W. Liu, A. Hagenbach, U. Abram, R. Gust. Synthesis, characterization and *in vitro* antitumour activity of a series of novel platinum (II) complexes bearing Schiff base ligands. Eur. J. Med. Chem. 53 (2012) 168 – 175.

[17] L. Li, C. Tian, C. Wang, G. Wang, L. Wang, J. Du. Platinum (II) complexes with tetradentate Schiff bases as ligands: Synthesis, characterization and detection of DNA interaction by differential pulse voltammetry. E-Journal of Chemistry 9 (3) (2012) 1422−1430.

[18] M. Azam, S. I. Al-Resayes, S. M. Soliman, A. Trzesowska-Kruszynska, R. Kruszynski, Z. Khan. A (salicyidiminato) Pt (II) complex with dimethylpropylene linkage: Synthesis, structural characterization and antineoplatic activity. J. Photochem. Photobiol. B: Biol. 176 (2017) 150-156.

[19] H. Naeimi, J. Safari, A. Heidarnezhad. Synthesis of Schiff base ligands derived from condensation of salicylaldehyde derivatives and synthetic diamine. Dyes and Pigments 73 (2007) 251−253.

[20] Quang Trung Nguyen, Quang Hai Lam, Van Tuyen Nguyen. Synthesis, characterization and *in vitro* antitumour activity of Pt (II) complexes of salen type Schiff base ligands. Vietnam J. Chem. 54 (6e2) (2016) 219−222.

[21] K. I. Ansari, J. D. Grant, S. Kasiri, G. Woldemariam, B. Shrestha, S. S. Mandal. Manganese (III)-salens induce tumor selective apoptosis in human cells. J. Inorg. Biochem. 103 (2009) 818–826.